Superconducting proximity effect and interface transparency in Nb/PdNi bilayers

C. Cirillo, S. L. Prischepa,* M. Salvato,† and C. Attanasio‡
Dipartimento di Fisica "E. R. Caianiello" and Laboratorio Regionale SuperMat INFM-Salerno, Università degli Studi di Salerno, Baronissi (Sa) I-84081, Italy

M. Hesselberth and J. Aarts
Kamerlingh Onnes Laboratory, Leiden University, P.O. Box 9504, 2300 RA Leiden, The Netherlands
(Received 11 April 2005; revised manuscript received 5 July 2005; published 14 October 2005)

The proximity effect between a superconductor (S) and a weak ferromagnet (F) in sputtered $Nb/Pd_{0.86}Ni_{0.14}$ bilayers has been studied. The dependence of the critical temperature on the S- and F-layer thicknesses can be interpreted in the framework of recent theoretical models and yields reasonable numbers for the exchange energy of the ferromagnet and the interface transparency of the S/F barrier.

DOI: 10.1103/PhysRevB.72.144511 PACS number(s): 74.45.+c, 74.78.Fk

I. INTRODUCTION

The investigation of the interplay of superconductivity and ferromagnetism in S/F hybrids is a very active area of research. The renewed interest in proximity effects in these systems is due both to the development of technology, which makes possible to fabricate heterostructures consisting of very thin layers, and to the intriguing physics behind them. Such S/F hybrid structures are important from a scientific point of view since they allow the investigation of the interplay between two antagonistic phenomena, superconductivity and ferromagnetism,[1,2] as well as the study of applications such as F/S/F spin valves[3,4] and S/F/S π-junctions.[5,6]

Here we will focus our attention on S/F bilayers. For these structures a nonmonotonic behavior of the critical temperature as a function of the thickness of the ferromagnetic layer has been found theoretically[7–11] as well as experimentally.[12,13] The presence of the exchange field E_{ex} in F causes an energy shift between the quasiparticles of the pair entering the ferromagnet and this results in the creation of Cooper pairs with nonzero momentum.[8] This implies that the superconducting order parameter does not simply decay in the ferromagnetic metal, as it happens in normal metals, but also oscillates over a length scale given by ξ_F, the coherence length in F. This length can be estimated from the dirty limit expression:[6]

$$\xi_F^{Dirty} = \sqrt{\frac{\hbar D_F}{E_{ex}}}, \quad (1)$$

where D_F is the diffusion coefficient of the F-metal. Qualitatively, the nonmonotonic behavior of the transition temperature can be seen as a consequence of the interference of quasiparticles (electrons and holes) that experience Andreev reflections at the S/F interface and normal reflections at the vacuum interface of the F layer. This interference can be constructive or destructive depending on the thickness d_F of the F layer[8–10] and can lead to oscillations of the superconducting transition temperature T_c as a function of d_F. Experimentally, such oscillations in F/S/F trilayers have been observed in systems involving, for instance, Fe or Co as ferromagnet,[14–16] and in the Fe/V system even re-entrant superconductivity.[17] However, in these systems with strong ferromagnets and exchange energies typically of the order of 1 eV, ξ_F^{Dirty} is of the order of 0.1–1 nm, which is very difficult to control experimentally. Furthermore, in this thickness range different complications can be present, such as interdiffusion or alloying effects, resulting in a magnetically dead layer,[12,14] or interfacial roughness,[18] all of which strongly influence the interface transparency, $\mathcal{T}$. This crucial parameter determines the strength of the proximity effect and is not directly measurable, but it is clear that the non-perfect transparency of the interfaces greatly reduces the amplitude of the order parameter oscillation,[9,10] which also explains why experiments on the same material combinations may yield different results.

For these reasons, systems where the F layer consists of a magnetic alloy whose exchange energy can be controlled by varying the amount of magnetic component, are of great interest. This is the case for $Pd_{1-x}Ni_x$ $(0<x<0.2)$, where E_{ex} can be varied in the meV range by changing the Ni concentration in the highly paramagnetic metallic matrix of Pd. In this system, ξ_F^{Dirty} is of the the order of 3–6 nm, a thickness accessible to standard deposition techniques. Another advantage of the $Nb/Pd_{1-x}Ni_x$ is that interdiffusion between the two layers will be limited by the bcc/fcc interface. It is also of interest to compare $Pd_{1-x}Ni_x$ to other weak ferromagnets such as $Cu_{1-x}Ni_x$, where weak oscillations in T_c were observed.[19,20] An extra reason to compare the two systems is that the Nb/Pd system possibly yields higher values of the interface transparency[21,22] than the ones based on Nb/Cu.[23]

In the present paper we present measurements of the superconducting critical temperatures of $Nb/Pd_{0.86}Ni_{0.14}$ bilayers and we extract parameters which describe this behavior. A brief description of the sample preparation and characterization and the results of the transport measurements are presented in Secs. II and III, respectively. In Sec. IV the experimental results are fitted in the framework of the theoretical model developed by Fominov[10] to derive microscopic proximity effect parameters, in particular the exchange energy of the ferromagnet and the transparency $\mathcal{T}$ of the $Nb/Pd_{0.86}Ni_{0.14}$ barrier. These values will be compared to the ones obtained for other S/F systems as well as for the correspondent S/N system, Nb/Pd, in Sec. V.

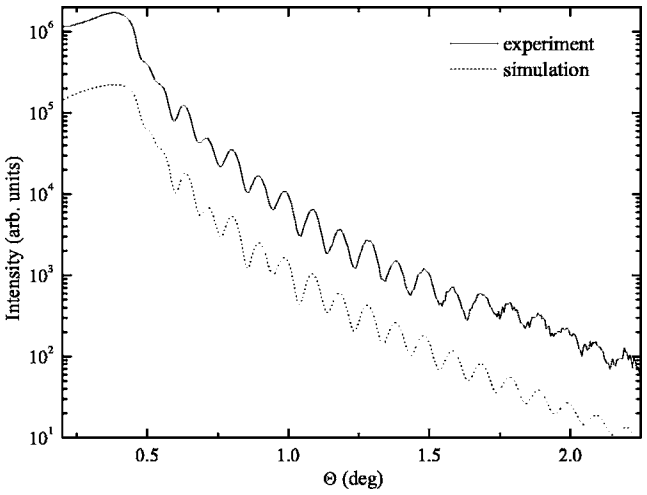

FIG. 1. Experimental (solid line) and calculated (dashed line) low-angle reflectivity profile for a $Nb/Pd_{0.86}Ni_{0.14}$ bilayer. The numerical simulation is arbitrarily shifted downward for sake of clearness.

II. SAMPLE PREPARATION AND CHARACTERIZATION

Bilayers of $Sub/Pd_{0.86}Ni_{0.14}/Nb$ (where Sub denotes the substrate) were grown in a dual source dc triode magnetron sputtering system on Si(100) substrates. A movable substrate holder allows to fabricate 8 different samples in a single deposition run. The deposition conditions were similar to those of the Nb/Pd multilayers described earlier.[21,24] Three different sets of bilayers were prepared. One set, with the Nb thickness d_{Nb} fixed at 35 nm, was deposited to study T_c as a function of the ferromagnetic layer thickness, d_{PdNi}. Two sets, consisting of a $Pd_{0.86}Ni_{0.14}$ layer with constant thickness ($d_{PdNi}=48.4$ nm) and a Nb layer with variable thickness ($d_{Nb}=10-150$ nm) were used to determine $T_c(d_{Nb})$ behavior. Moreover, one set of single Nb films with different thicknesses was deposited, in order to study the intrinsic suppression of the critical temperature with the Nb thickness. Single $Pd_{0.86}Ni_{0.14}$ films were also grown to study the magnetic properties of the alloy.

In the fabrication of artificially layered structures for the study of proximity effect, attention must be paid to interface properties. In particular, in order to have transparent barriers the existence of flat layers and of interfaces with small roughness is essential. For this reason the interface quality was studied by x-ray reflectivity measurements, using a Philips X-Pert MRD high resolution diffractometer. The x-ray reflectivity analysis was performed on bilayers deliberately fabricated with appropriate thicknesses under the same conditions as for the samples used in superconductivity measurements. The reflectivity profile of a $Sub/Nb/Pd_{0.86}Ni_{0.14}$ bilayer with $d_{Nb}=18.0$ nm and $d_{PdNi}=23.7$ nm is shown in Fig. 1 together with the simulation curve obtained using the Parrat and Nevot–Croce formalism.[25,26] The fit reveals that the bottom Si/Nb interface has a roughness value of 1.2 nm, while the top $Nb/Pd_{0.86}Ni_{0.14}$ interface has a smaller roughness of about 0.7 nm. The film thicknesses obtained from the simulation were used for the final calibration of d_{Nb} and d_{PdNi}.

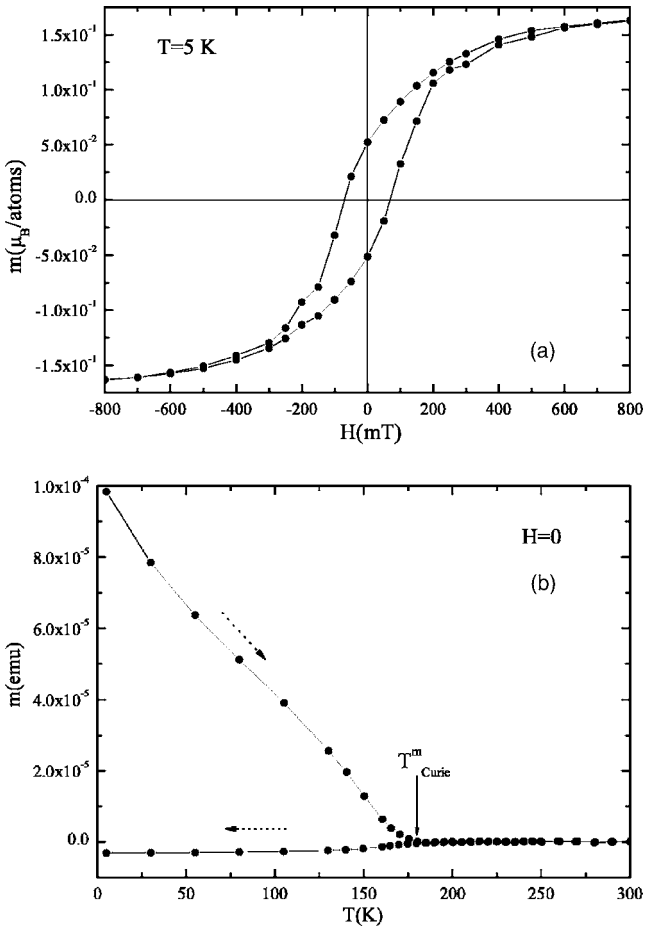

FIG. 2. (a) Magnetization loop for a single $Pd_{0.86}Ni_{0.14}$ film at $T=5$ K. (b) Magnetic moment as a function of the temperature for the same film, after saturation at $T=5$ K. The dotted arrows indicate the measurement sequence.

The onset of ferromagnetism in $Pd_{1-x}Ni_x$ alloys is around $x=0.023$.[27] In order to have magnetic homogeneity a $Pd_{1-x}Ni_x$ target with $x=0.10$ was used. This stoichiometry was not conserved in the samples as revealed by the Rutherford backscattering analysis, which gives a Ni concentration of $x=0.14$. The hysteresis loop of a $Pd_{0.86}Ni_{0.14}$ single film, 48.4 nm thick, is presented in Fig. 2(a). The measurements were performed by a SQUID magnetometer at a temperature of 5 K with the surface of the sample parallel to the magnetic field. At this temperature the value of the saturation magnetic moment is $m_{sat}=0.17$ μ_B/atom, while the coercive field is about 70 mT. For the same sample, the temperature dependence of the magnetic moment m was measured, in order to derive the value of the Curie temperature, T^m_{Curie}. The sample was magnetized to saturation at 5 K, the field was then removed and m(T) was measured up to 300 K and down again to 5 K. T^m_{Curie} was defined as the point where irreversibility appears when cooling down the sample, and was estimated to be $T^m_{Curie}=185$ K. Also the resistance R of the sample was measured between 300 K and 4 K, as shown in Fig. 3. A clear shoulder is observed around 210 K. The connection to the magnetic ordering becomes more clear from the behavior of the derivative of R with respect to T, $dR(T)/dT$, plotted in the insert. Between 300 K and 220 K, $dR(T)/dT$ decreases,

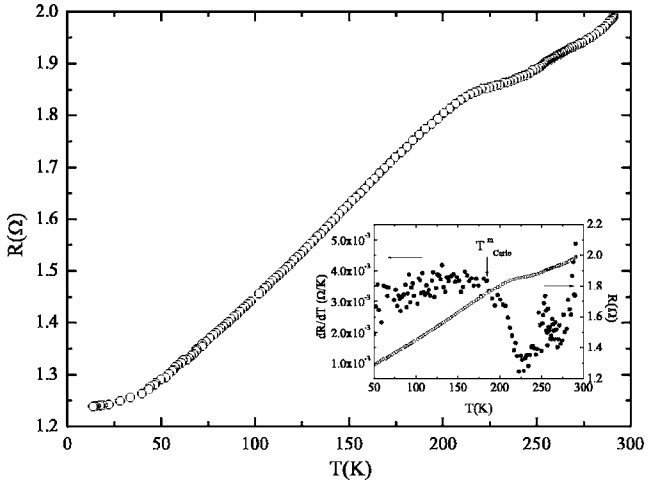

FIG. 3. Electrical resistance as a function of temperature for a PdNi single film, 48.4 nm thick. Inset: magnification of the main panel data (open symbols) compared with its first derivative (closed symbols). The arrow indicates the value of the Curie temperature derived from the $m(T)$ measurement.

followed by a steep rise between 220 K and 190 K, after which $dR(T)/dT$ flattens. The behavior can be compared to that of magnetic ordering in other metallic systems,[28] where the minimum in $dR(T)/dT$ is due to short-range fluctuations just above T_{Curie}, while T_{Curie} itself is found at the maximum below the steep rise. If we simply define T^{R}_{Curie} as the temperature where the rise flattens, we find $T^{R}_{\mathrm{Curie}} \approx 200$ K, in reasonable agreement with T^{m}_{Curie}.

III. SUPERCONDUCTING PROPERTIES

The superconducting transition temperatures T_c were resistively measured using a standard dc four-probe technique. T_c was defined as the midpoint of the transition curve. In Fig. 4, examples are presented of such transitions for some samples from both the series with variable PdNi thickness d_{PdNi} and with variable Nb thickness d_{Nb}, respectively. In the first case, the widths of the transitions never exceeded 0.1 K, while for the series with variable Nb thickness they were typically less than 0.2 K. The measured values of the Nb resistivity of samples 200 nm and 35 nm thick, were 6 $\mu\Omega$ cm and 17 $\mu\Omega$ cm, respectively. The electrical resistivity of a 30 nm PdNi film was $\rho_{\mathrm{PdNi}}=24$ $\mu\Omega$ cm, while the resistivity of thinner PdNi films between 1–9 nm was around 50 $\mu\Omega$ cm.

In Fig. 5 the dependence of the superconducting transition temperature on the thickness of the PdNi layer, with d_{Nb} fixed at 35 nm, is shown. The bulk value $T_{cS}=7$ K is the transition temperature of a single Nb film with $d_{\mathrm{Nb}}=35$ nm. Increasing d_{F}, T_c exhibits a rapid drop, until a saturation value is obtained.

The dependence of the critical temperatures T_c on the thickness of the Nb layer d_{Nb}, with d_{PdNi} fixed at 48.4 nm, is shown in Fig. 6. The transition temperature of the sample with $d_{\mathrm{Nb}}=15$ nm is not reported since it was below 1.8 K, the lowest temperature reachable with our experimental setup. In

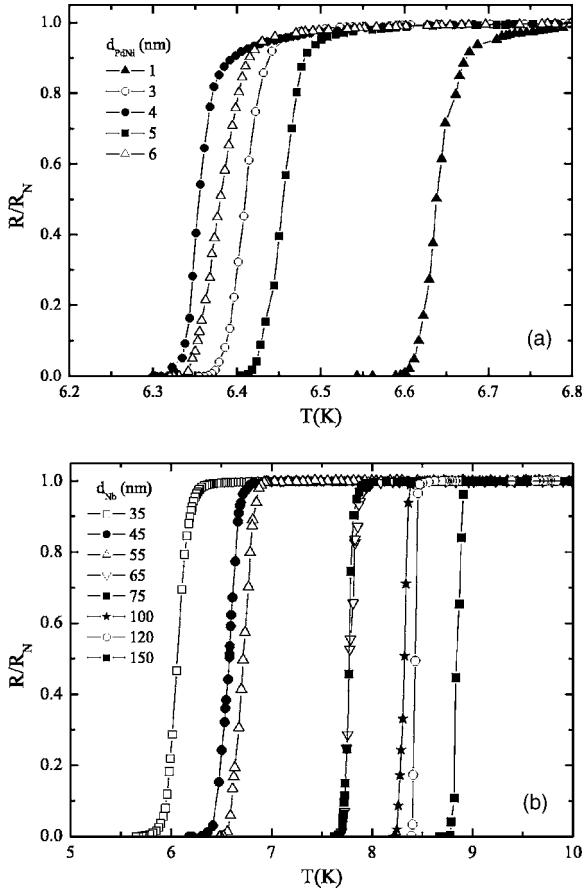

FIG. 4. Resistive transitions $R(T)$ normalized respect to $R_N = R(10\ \mathrm{K})$ for some of the measured samples from the different sets: (a) series with constant Nb thickness $d_{\mathrm{Nb}}=35$ nm and variable PdNi thickness, $d_{\mathrm{PdNi}}=1-3-4-5-6$ nm; (b) series with constant PdNi thickness $d_{\mathrm{PdNi}}=48.4$ nm and variable Nb thickness, $d_{\mathrm{Nb}}=35-45-55-65-75-100-120-150$ nm.

Fig. 6, the critical temperatures $T_c(d_{\mathrm{Nb}})$ are compared to those of single Nb films (open symbols), indicating that the suppression of the superconducting transition temperature of Nb/PdNi bilayer is due to the proximity effect rather than to the intrinsic thickness dependence of the single Nb. The last is described by the phenomenological relation:

$$T_c(d_{\mathrm{Nb}}) = T_{c0}(1 - d_0/d_{\mathrm{Nb}}) \tag{2}$$

with $T_{c0}=9.2$ K and d_0 the minimum thickness of the Nb film with T_c different from zero. The dotted curve in Fig. 6 is obtained for $d_0=8$ nm.

IV. ANALYSIS OF THE DATA

This section deals with the interpretation of the experimental results, by fitting them in the framework of a theoretical model which explicitly takes into account the exchange energy of the ferromagnet E_{ex} and the interface transparency $\mathcal{T}$. The first well known theory for S/F proximity effect was the one by Radovic.[29] However, even though it well describes the behavior of critical temperatures and critical fields, this theory assumes a perfect interface, a condition

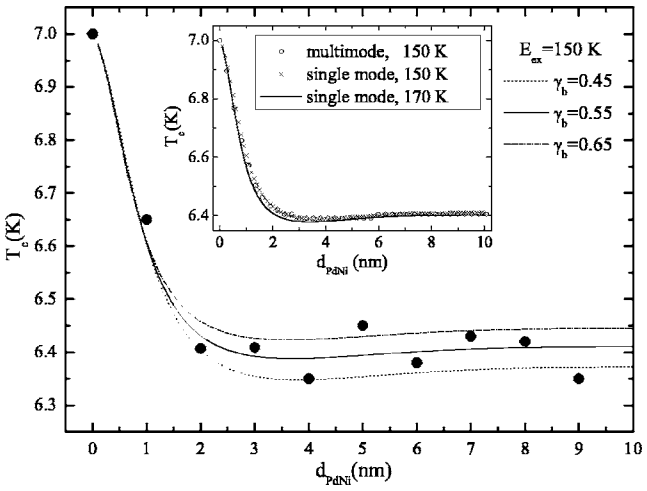

FIG. 5. The critical temperature T_c versus PdNi thickness d_{PdNi} in $\mathrm{Nb/Pd_{0.86}Ni_{0.14}}$ bilayers with constant Nb thickness $d_{\mathrm{Nb}}=35$ nm. Different lines (dotted, solid, and dot-dashed) are the results of the theoretical fit in the single mode approximation for different values of γ_b. The insert shows a comparison between the single mode (○) and the multimode (×) calculations for $E_{\mathrm{ex}}=150$ K. The drawn line is a single mode calculation for $E_{\mathrm{ex}}=170$ K.

which is never fulfilled in real systems. $\mathcal{T}$ is a parameter which describes the resistance experienced by electrons crossing the barriers between two metals. Interface imperfections, mismatches between Fermi velocities and band structure of the two metals all act as a potential barrier at the interface, that screens the proximity effect. These are the

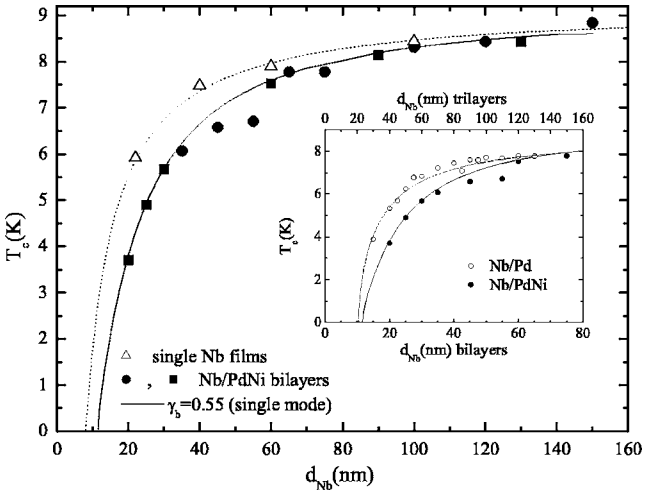

FIG. 6. The critical temperature T_c versus Nb thickness d_{Nb} in $\mathrm{Nb/Pd_{0.86}Ni_{0.14}}$ bilayers with constant PdNi thickness $d_{\mathrm{PdNi}}=48.4$ nm. Different closed symbols refer to samples sets obtained in different deposition runs. Open symbols refers to single Nb films. The dotted line describes the phenomenological T_c thickness dependence of Nb single films. The solid line is the result of the theoretical calculations in the single mode approximation. The fitting parameters are given in the text. Inset: $T_c(d_{\mathrm{Nb}})$ curves for Nb/Pd (open symbols) and Nb/PdNi (closed symbols). The solid and the dot-dashed lines indicate the results of the theoretical calculation reported above and in Ref. 21, respectively.

possible causes of the reduction of $\mathcal{T}$ in S/N systems. At the S/F barrier the transparency can undergo an additional decrease, due to the polarization of the conduction electrons in the ferromagnet and to the spin dependent impurity scattering.[30,31]

The theoretical model developed by Fominov,[10] considered in this paper, takes a weak exchange field and the finite transparency of the interfaces explicitly into account. Moreover, this theory was already applied in the case of another weak ferromagnetic alloy, namely $\mathrm{Nb/Cu_{0.43}Ni_{0.57}}$, while the analogous model developed by Tagirov,[9] formulated in terms of a clean regime (long mean free path, $l_F > \xi_F$) is more suited for strong ferromagnets. The starting point of Fominov's model are the linearized Usadel equation,[32] with the boundary conditions derived by Kupriyanov and Lukichev[33] for the pairing function at the outer surfaces of the bilayers:

$$\frac{dF_S(d_S)}{dx} = \frac{dF_F(-d_F)}{dx} = 0 \tag{3}$$

as well as at the S/F boundary:

$$\xi_S \frac{dF_S(0)}{dx} = \gamma \xi_F^* \frac{dF_{\mathrm{F}}(0)}{dx}, \quad \gamma = \frac{\rho_S \xi_S}{\rho_F \xi_F^*}, \tag{4}$$

$$\xi_F^* \gamma_b \frac{dF_F(0)}{dx} = F_S(0) - F_F(0), \quad \gamma_b = \frac{R_B \mathcal{A}}{\rho_F \xi_F^*}, \tag{5}$$

where

$$\xi_S = \sqrt{\frac{\hbar D_S}{2\pi k_B T_{cS}}}, \tag{6}$$

$$\xi_F^* = \sqrt{\frac{\hbar D_{\mathrm{F}}}{2\pi k_B T_{cS}}}. \tag{7}$$

Here $\rho_{\mathrm{S,F}}$ and $D_{\mathrm{S,F}}$ are the low temperature resistivities and the diffusion coefficients of S and F, respectively, while R_B is the normal-state boundary resistivity and $\mathcal{A}$ is its area. Note that ξ_F^* does not depend on E_{ex}, and is therefore not the same as ξ_F^{Dirty}. The parameter γ is a measure of the strength of the proximity effect between the S and F metals while γ_b describes the effect of the interface transparency $\mathcal{T}$. In this model $\mathcal{T}$ is defined as:

$$\gamma_b = \frac{2}{3}\frac{l_F}{\xi_F^*}\frac{1-\mathcal{T}}{\mathcal{T}}. \tag{8}$$

$\mathcal{T}$ is zero for the completely reflecting interface (large resistance of the barrier R_B) and it is equal to one for a completely transparent one. It is useful to compare this definition to the T_m present in Tagirov's model[9] and reported in a number of experiments.[13,15,17,44] The two definitions are linked through the expression:

$$T_m = \frac{\mathcal{T}}{1-\mathcal{T}}, \tag{9}$$

where this time T_m can vary between zero (negligible transparency) and infinity (perfect interface).

It is important to note that the boundary condition (5) determines a jump of the pairing function at the interface, in contrast with Radovic's picture, in which, due to the perfect boundary, the pairing function varies continuously.

The above problem can be solved analytically only in limiting cases. One of them, often used, is the single-mode approximation. In this case the critical temperature of the bilayer is determined by the equations:

$$\ln\left(\frac{T_{cS}}{T_c}\right) = \Psi\left(\frac{1}{2} + \frac{\Omega_n^2}{2}\frac{T_{cS}}{T_c}\right) - \Psi\left(\frac{1}{2}\right), \tag{10}$$

$$\Omega_n \tan\left(\Omega_n \frac{d_S}{\xi_S}\right) = W(\omega_n), \tag{11}$$

with

$$W(\omega_n) = \gamma \frac{A_S(\gamma_b + ReB_F) + \gamma}{A_S|\gamma_b + B_F|^2 + \gamma(\gamma_b + ReB_F)}, \tag{12}$$

$$B_F = [k_F \xi_F^* \tanh(k_F d_F)]^{-1}, \quad k_F = \frac{1}{\xi_F^*}\sqrt{\frac{|\omega_n| + iE_{ex}\,\mathrm{sgn}\,\omega_n}{\pi k_B T_{cS}}}, \tag{13}$$

$$A_S = k_S \xi_S \tanh(k_S d_S), \quad k_S = \frac{1}{\xi_S}\sqrt{\frac{\omega_n}{\pi k_B T_{cS}}}. \tag{14}$$

where $\omega_n = \pi T_c(2n+1)$ with $n = 0, \pm 1, \pm 2, \ldots$ are the Matsubara frequencies, $\Psi(x)$ is the digamma function and T_{cS} is the critical temperature of the single S layer.

In this approximation only the real root Ω_0 of Eq. (10) is taken into account, while the other imaginary roots are neglected. The exact multi-mode solution is obtained by taking also the imaginary roots of Ω into account. As shown by Fominov[10] in the general case the results of the two calculations can be different and the single-mode method is applicable only if the experimental parameters are such that W can be considered ω_n independent. In particular in the case when $E_{ex}/\pi T_{cS} > 1$ and $d_F \sim \xi_F$ the method is valid if $\sqrt{E_{ex}/(\pi T_{cs})} \gg 1/\gamma_b$. We shall use the single-mode approximation and compare it to the full (multi-mode) calculation.[34]

A large number of microscopic parameters appears in Eqs. (10)–(14). However, part of them can be derived independently. The electrical resistivities were determined experimentally. The Nb coherence length, ξ_S, can be determined through the expression (6), where the diffusion coefficient D_S is related to the low temperature resistivity ρ_S through the electronic mean free path l_S by Ref. 35

$$D_S = \frac{v_S l_S}{3} \tag{15}$$

in which

$$l_S = \frac{1}{v_S \gamma_S \rho_S}\left(\frac{\pi k_B}{e}\right)^2, \tag{16}$$

where $\gamma_S \equiv \gamma_{Nb} \approx 7 \times 10^{-4}$ J/K^2 cm^3 is the Nb electronic specific heat coefficient[36] and $v_S \equiv v_{Nb} = 2.73 \times 10^7$ cm/s is the Nb Fermi velocity.[37] In this way the value obtained for the mean free path and for the coherence length of the single Nb film of the series with variable PdNi thickness, 35 nm thick, with $T_{cS} = 7$ K and $\rho_{Nb} = 17\ \mu\Omega$ cm are $l_{Nb} \approx 2.3$ nm and $\xi_{Nb} \approx 6$ nm, respectively. The coherence length ξ_F^* is determined according to Eq. (7). As we found that the resistance of the F layers depends on thickness below 30 nm, we assume that the PdNi mean free path is thickness-limited and use an average value of $l_F \approx 4$ nm; together with the Pd Fermi velocity $v_F \equiv v_{Pd} = 2.00 \times 10^7$ cm/s (Ref. 38) this leads to a value of $\xi_F^* = 6.8$ nm. In this way E_{ex} and γ_b are used as the only free parameters in the theory. The fitting procedure consisted in determining E_{ex} value where T_c starts to saturate as function of d_{PdNi}, while γ_b was used to control of the vertical position of the curve.

The solid line in Fig. 5 is obtained as the result of the calculations for $E_{ex} = 150$ K and $\gamma_b = 0.55$, with the fixed parameters $d_{Nb} = 35$ nm, $T_{cS} = 7$ K, $\xi_{Nb} = 6$ nm, $\xi_{PdNi}^* = 6.8$ nm, $\rho_{PdNi} = 50\ \mu\Omega$ cm, and $\rho_{Nb} = 17\ \mu\Omega$ cm. The fits are quite insensitive to the value of E_{ex}, as can be seen in the insert, where a curve with $E_{ex} = 170$ K is displayed for comparison. A reasonable error bar is $E_{ex} = 150\ \mathrm{K} \pm 20$ K. Theoretical fits for different values of γ_b are also given, and show that the fits are quite sensitive to the value of γ_b.

The formation of a possible Nb oxide layer at the top of the bilayers was also considered. An oxide layer 1.5 nm thick, and the consequent reduction of the effective Nb layer, would affect the theoretical fit, leading to a value of $\gamma_b = 0.65$. This effect, together with the dispersion of the experimental points, allows to estimate an error bar of $\gamma_b = 0.60 \pm 0.15$.

From the data in Fig. 5, a good estimate can be obtained for ξ_F^{Dirty}. As can be inferred from the calculations presented in Ref. 10, this parameter is phenomenologically related to the position of the minimum in $T_c(d_F)$ according to $d_{min} = 0.7\pi\xi_F^{Dirty}/2$. With $d_{min} \approx 3.8$ nm, we find $\xi_F^{Dirty} \approx 3.4$ nm, in very good agreement with the value of 3.7 nm which can be obtained from Eq. (1). The insert of Fig. 5 also shows a comparison of the single mode and the full multimode calculation. This is reasonable in view of the fact that the limit of applicability of the single mode calculation $\sqrt{E_{ex}/(\pi T_{cs})}$ (≈ 3) $\gg 1/\gamma_b$ (≈ 2) is fulfilled.

With the same set of equations the behavior of $T_c(d_{Nb})$ was also reproduced. In the theoretical calculations the intrinsic critical temperature dependence of the single Nb films was taken into account through relation (2). The solid line in Fig. 6 represents the model calculation obtained using the values for E_{ex} and γ_b obtained from the $T_c(d_{PdNi})$ fit, and the fixed parameter values $T_{cS} = 7$ K, $\xi_{Nb} = 6$ nm, $\xi_{PdNi}^* = 6.8$ nm, $\rho_{PdNi} = 24\ \mu\Omega$ cm, $\rho_{Nb} = 17\ \mu\Omega$ cm. The theory and the experimental data are in very good agreement. Again, the multimode calculation yielded results which cannot be discerned from the single mode calculations.

V. DISCUSSION AND CONCLUSIONS

The superconducting critical temperatures behavior of $Nb/Pd_{0.86}Ni_{0.14}$ was studied in two different approximations the single-mode and the multi-mode methods, which both

give the same final results. The fits to the two sets of data, $T_c(d_{\mathrm{PdNi}})$ and $T_c(d_{\mathrm{Nb}})$, give us confidence to conclude that for our $\mathrm{Nb/Pd_{0.86}Ni_{0.14}}$ bilayers, $E_{\mathrm{ex}} \approx 150\ \mathrm{K} \pm 20\ \mathrm{K}$ (=13 meV ±2 meV) and $\gamma_b \approx 0.60 \pm 0.15$, which means $\mathcal{T} \approx 0.39$. Note that the value for E_{ex} is derived for relatively thin layers of $\mathrm{Pd_{0.86}Ni_{0.14}}$, and that the bulk value may be a little bit higher. The value obtained for the parameter γ_b is of the same order of magnitude as found in other S/N systems, and also as in $\mathrm{Nb/Cu_{0.43}Ni_{0.57}}$.[10,39] It is much lower than values obtained in the framework of similar models based on the linearized Usadel equations for the traditional S/F systems, such as V/Fe and Nb/Fe where $\gamma_b = 80$ (Ref. 41) and $\gamma_b = 42$ (Ref. 40) were found. It shows once again that in weak ferromagnets such as $\mathrm{Pd_{1-x}Ni_x}$ ($x \approx 0.1$) or $\mathrm{Cu_{1-x}Ni_x}$ ($x \approx 0.5$) there is no appreciable change in the barrier transparency due to the suppression of Andreev reflections by the splitting of the spin subbands. At this point, we find it difficult to compare the results for the transparency with those previously obtained for the corresponding nonmagnetic Nb/Pd system,[21,22] in particular because in that analysis no possible effects of spin fluctuation were taken into account. As was shown recently, the superconducting gap induced in Pd is significantly smaller than the gap induced for instance in Ag, and the difference can be explained by taking into account the unusually large Stoner factor for Pd.[42] This should also play a role in the T_c-variations in Nb/Pd. In that respect it is interesting to note that the value of $d_{\mathrm{Nb}}^{\mathrm{cr}}$ is rather high. For the present $\mathrm{Nb/Pd_{0.86}Ni_{0.14}}$ bilayers we find $d_{\mathrm{Nb}}^{\mathrm{cr}} = 11.6$ nm, yielding $d_{\mathrm{Nb}}^{\mathrm{cr}}/\xi_{\mathrm{Nb}} = 1.45$, which corresponds to 2.9 for the trilayers case. For the Nb/Pd trilayers (see inset of Fig. 6), the number was $d_{\mathrm{Nb}}^{\mathrm{cr}} = 20$ nm, or $d_{\mathrm{Nb}}^{\mathrm{cr}}/\xi_{\mathrm{Nb}} = 3.1$, a very similar value. This value is lower than the ones reported for traditional S/F systems[43,44] (around 4.5), but significantly higher than the values around 1.6 reported for other systems with weak ferromagnets, namely $\mathrm{Nb/Cu_{1-x}Ni_x}$ trilayers with $x = 0.67$, 0.59, and 0.52.[20] It suggests that the Pd-based systems show relatively strong pair breaking and/or relatively high interface transparency.

A final comparison can be made with density-of-states measurements[5,42] and critical current measurements[45] on $\mathrm{Nb/Pd_{1-x}Ni_x}$ ($x \approx 0.12$). The values for E_{ex} are mostly similar, in the range 10–15 meV, although the value of 35 meV extracted from the critical current data appears too high. More surprising is the large difference in the value for γ_b of the order of 5, which is used to describe those measurements. It would not be possible to describe the present proximity effect measurements with such a low value for the interface transparency. This is an important conclusion of the present work. At the moment, the $\mathrm{Nb/Pd_{1-x}Ni_x}$ system is the only one where both data from Josephson junctions and perpendicular transport, as well as data from bilayer *Tc*'s are available. For both data sets a quantitative description is now available, in terms of the same theoretical framework, but they come to widely different conclusions with regard to the S/F interface. It signals that, even though the theoretical descriptions look adequate, a possibly important part of the physics may be missed.

ACKNOWLEDGMENTS

We would like to thank A. A. Golubov and Ya. V. Fominov for useful discussions, and the latter also for making his computer code for the multi-mode calculations available to us.

*Permanent address: State University of Informatics and Radioelectronics, P. Brovka Street 6, 220013 Minsk, Belarus.

†Present address: Dipartimento di Fisica, Università di Roma "Tor Vergata," Via della Ricerca Scientifica, I-00133 Roma, Italy.

‡Corresponding author. Tel. +39-089-965288, Fax +39-089-965275, e-mail: attanasio@sa.infn.it

[1] P. Fulde and R. A. Ferrell, Phys. Rev. **135**, A550 (1964).

[2] A. I. Larkin and Yu. N. Ovchinnikov, Sov. Phys. JETP **20**, 762 (1965).

[3] L. R. Tagirov, Phys. Rev. Lett. **83**, 2058 (1999).

[4] A. I. Buzdin, A. V. Vedyayev, and N. V. Ryzhanova, Europhys. Lett. **48**, 686 (1999).

[5] T. Kontos, M. Aprili, J. Lesueur, and X. Grison, Phys. Rev. Lett. **86**, 304 (2001).

[6] V. V. Ryazanov, V. A. Oboznov, A. Yu. Rusanov, A. V. Veretennikov, A. A. Golubov, and J. Aarts, Phys. Rev. Lett. **86**, 2427 (2001).

[7] M. G. Khusainov and Yu. N. Proshin, Phys. Rev. B **56**, R14283 (1997).

[8] E. A. Demler, G. B. Arnold, and M. R. Beasley, Phys. Rev. B **55**, 15174 (1997).

[9] L. R. Tagirov, Physica C **307**, 145 (1998).

[10] Ya. V. Fominov, N. M. Chtchelkatchev, and A. A. Golubov, Phys. Rev. B **66**, 014507 (2002).

[11] A. Bagrets, C. Lacroix, and A. Vedyayev, Phys. Rev. B **68**, 054532 (2003).

[12] Th. Mühge, K. Theis-Bröhl, K. Westerholt, H. Zabel, N. N. Garif'yanov, Yu. V. Goryunov, I. A. Garifullin, and G. G. Khaliullin, Phys. Rev. B **57**, 5071 (1998).

[13] A. S. Sidorenko, V. I. Zdravkov, A. A. Prepelitsa, C. Helbig, Y. Luo, S. Gsell, M. Schreck, S. Klimm, S. Horn, L. R. Tagirov, and R. Tidecks, Ann. Phys. **12**, 37 (2003).

[14] Th. Mühge, N. N. Garif'yanov, Yu. V. Goryunov, G. G. Khaliullin, L. R. Tagirov, K. Westerholt, I. A. Garifullin, and H. Zabel, Phys. Rev. Lett. **77**, 1857 (1996).

[15] I. A. Garifullin, D. A. Tikhonov, N. N. Garifyanov, M. Z. Fattakhov, L. R. Tagirov, K. Theis-Bröhl, K. Westerholt, and H. Zabel, Phys. Rev. B **70**, 054505 (2004), and references therein.

[16] Y. Obi, M. Ikebe, and H. Fujishiro, Phys. Rev. Lett. **94**, 057008 (2005).

[17] I. A. Garifullin, D. A. Tikhonov, N. N. Garifyanov, L. Lazar, Yu. V. Goryunov, S. Ya. Khlebnikov, L. R. Tagirov, K. Westerholt, and H. Zabel, Phys. Rev. B **66**, 020505(R) (2002).

[18] N. N. Garifyanov, Yu. V. Goryunov, Th. Mühge, L. Lazar, G. G. Khaliullin, K. Westerholt, I. A. Garifullin, and H. Zabel, Eur. Phys. J. B **1**, 405 (1998).

[19] V. V. Ryazanov, V. A. Oboznov, A. S. Prokofiev, and S. V. Dubonos, JETP Lett. **77**, 39 (2003).

[20] A. Rusanov, R. Boogaard, M. Hesselberth, H. Sellier, and J. Aarts, Physica C **369**, 300 (2002).
[21] C. Cirillo, S. L. Prischepa, M. Salvato, and C. Attanasio, Eur. Phys. J. B **38**, 59 (2004).
[22] C. Cirillo, S. L. Prischepa, A. Romano, M. Salvato, and C. Attanasio, Physica C **404**, 95 (2004).
[23] A. Tesauro, A. Aurigemma, C. Cirillo, S. L. Prischepa, M. Salvato, and C. Attanasio, Supercond. Sci. Technol. **18**, 1 (2005).
[24] C. Cirillo, C. Attanasio, L. Maritato, L. V. Mercaldo, S. L. Prischepa, and M. Salvato, J. Low Temp. Phys. **130**, 509 (2003).
[25] L. G. Parrat, Phys. Rev. **95**, 359 (1954).
[26] L. Nevot and P. Croce, Rev. Phys. Appl. **15**, 761 (1980).
[27] A. Tari and B. R. Coles, J. Phys. F: Met. Phys. **1**, L69 (1971).
[28] M. P. Kawatra, J. I. Budnick, and J. A. Mydosh, Phys. Rev. B **2**, 1587 (1970).
[29] Z. Radovic, M. Ledvij, L. Dobrosavljevic-Grujic, A. I. Buzdin, and J. R. Clem, Phys. Rev. B **44**, 759 (1991).
[30] M. J. M. de Jong and C. W. J. Beenakker, Phys. Rev. Lett. **74**, 1657 (1995).
[31] S. K. Upádhyay, A. Palanisami, R. N. Louie, and R. A. Buhrman, Phys. Rev. Lett. **81**, 3247 (1998).
[32] K. Usadel, Phys. Rev. Lett. **25**, 507 (1970).
[33] M. Yu. Kupriyanov and V. F. Lukichev, Sov. Phys. JETP **67**, 1163 (1988).
[34] For this we used a computer code made available by Ya. V. Fominov.
[35] J. J. Hauser, H. C. Theurer, and N. R. Werthamer, Phys. Rev. **136**, A637 (1964).
[36] *Handbook of Chemistry and Physics*, edited by R. C. Weast (The Chemical Rubber Co., Cleveland, 1972).
[37] H. R. Kerchner, D. K. Christen, and S. T. Sekula, Phys. Rev. B **24**, 1200 (1981).
[38] L. Dumoulin, P. Nedellec, and P. M. Chaikin, Phys. Rev. Lett. **47**, 208 (1981).
[39] H. Sellier, Ph.D. Thesis, Université Grenoble I, 2002.
[40] J. M. E. Geers, M. B. S. Hesselberth, J. Aarts, and A. A. Golubov, Phys. Rev. B **64**, 094506 (2001).
[41] J. Aarts, J. M. E. Geers, E. Brück, A. A. Golubov, and R. Coehoorn, Phys. Rev. B **56**, 2779 (1997).
[42] T. Kontos, M. Aprili, J. Lesueur, X. Grison, and L. Dumoulin, Phys. Rev. Lett. **93**, 137001 (2004).
[43] Th. Mühge, K. Westerholt, H. Zabel, N. N. Garifyanov, Yu. V. Goryunov, I. A. Garifullin, and G. G. Khaliullin, Phys. Rev. B **55**, 8945 (1997).
[44] L. Lazar, K. Westerholt, H. Zabel, L. R. Tagirov, Yu. V. Goryunov, N. N. Garif'yanov, and I. A. Garifullin, Phys. Rev. B **61**, 3711 (2000).
[45] T. Kontos, M. Aprili, J. Lesueur, F. Genet, B. Stephanidis, and R. Boursier, Phys. Rev. Lett. **89**, 137007 (2002).